

Involvement of ERK1/2 activation in the gene expression of senescence-associated secretory factors in human hepatic stellate cells

Naoshi Odagiri, Tsutomu Matsubara, Moe Higuchi, Sayuri Takada, Hayato Urushima, Misako Sato-Matsubara, Yuga Teranishi, Katsutoshi Yoshizato, Norifumi Kawada, Kazuo Ikeda

Citation	Molecular and Cellular Biochemistry, 455(1-2); 7-19
Issue Date	2019-05-15
Type	Journal Article
Textversion	Author
Rights	This is a post-peer-review, pre-copyedit version of an article published in Molecular and Cellular Biochemistry. The final authenticated version is available online at: https://doi.org/10.1007/s11010-018-3466-x . See Springer Nature terms of use. https://www.springer.com/gp/open-access/publication-policies/aam-terms-of-use .
DOI	10.1007/s11010-018-3466-x

Self-Archiving by Author(s)
Placed on: Osaka City University

1
2
3 Title : Involvement of ERK1/2 activation in the gene expression of senescence-associated
4
5
6 secretory factors in human hepatic stellate cells.
7
8
9

10
11
12 Naoshi Odagiri^{1,2}, Tsutomu Matsubara^{1,*}, Moe Higuchi¹, Sayuri Takada^{1,2}, Hayato Urushima¹,
13
14
15
16 Misako Sato-Matsubara^{2,3}, Yuga Teranishi², Katsutoshi Yoshizato^{3,4}, Norifumi Kawada², Kazuo
17
18
19 Ikeda¹.
20
21
22
23
24

- 25
26 1. Department of Anatomy and Regenerative Biology, Osaka City University Graduate School
27
28 of Medicine, Osaka, 545-8585, Japan
29
30
31
32 2. Department of Hepatology, Osaka City University Graduate School of Medicine, Osaka,
33
34 545-8585, Japan.
35
36
37
38 3. Endowed Laboratory of Synthetic Biology, Osaka City University Graduate School of
39
40
41 Medicine, Osaka, 545-8585, Japan
42
43
44
45 4. Academic advisor's office of PhoenixBio Co. Ltd, Higashihiroshima, 739-0046, Japan
46
47
48
49
50

51 ***Correspondence:** Tsutomu Matsubara, Department of Anatomy and Regenerative Biology,
52
53
54 Osaka City University Graduate School of Medicine, Osaka, 545-8585, Japan, Tel: +81-6-6645-
55
56
57 3701, Fax: +81-6-6645-3702, Email: matsu335@med.osaka-cu.ac.jp
58
59
60

1
2
3 **Abstract**
4
5

6 Senescent hepatic stellate cells (senescent HSCs) are found in patients with liver cirrhosis
7
8
9 and have been thought to be involved in the development of hepatocellular carcinoma (HCC) in
10
11
12 mice via the senescence-associated secretory proteins. However, in humans, which secretory
13
14
15 proteins are involved and what regulate their expression remain unclear. In the current study, we
16
17
18 characterized senescence-associated β -galactosidase-positive senescent human HSCs (hHSCs)
19
20
21 induced by repetitive passaging. They exhibited enhanced expression of 14 genes for secretory
22
23
24 protein and persistent phosphorylation of ERK1/2 protein but not JNK or p38 MAPK proteins.
25
26
27 Enhanced nuclear ERK1/2 phosphorylation was observed in senescent hHSCs. Treatment of the
28
29
30 senescent hHSCs with ERK1/2 inhibitor, SCH772984, significantly decreased the levels of
31
32
33 angiopoietin like 4 (ANGPTL4), C-C motif chemokine ligand 7 (CCL7), Interleukin-8 (IL-8),
34
35
36 platelet factor 4 variant 1 (PF4V1), and TNF superfamily member 15 (TNFSF15) mRNA levels
37
38
39 in a dose-dependent manner. The enhanced phosphorylation of ERK1/2 and expression of
40
41
42 *ANGPTL4*, *IL-8* and *PF4V1* genes were observed in both of senescent human dermal fibroblasts
43
44
45 and X-ray-induced senescent hHSCs. However, transient ERK1/2 activation induced by
46
47
48 epidermal growth factor could not mimic the gene profile of the senescent hHSCs. These results
49
50
51 revealed involvement of ERK1/2 signalling in the regulation of senescence-associated secretory
52
53
54 factors, suggesting that simultaneous induction of *ANGPTL4*, *IL-8*, and *PF4V1* genes is a marker
55
56
57
58
59
60
61
62
63
64
65

1
2
3
4
5
6
7
8
9
10
11
12
13
14
15
16
17
18
19
20
21
22
23
24
25
26
27
28
29
30
31
32
33
34
35
36
37
38
39
40
41
42
43
44
45
46
47
48
49
50
51
52
53
54
55
56
57
58
59
60
61
62
63
64
65

of hHSC senescence. This study will contribute to understanding roles of senescent hHSCs in liver diseases.

Keywords

Hepatic stellate cell; Senescence; Secretory factor; ERK1/2; Fibroblast

1
2
3 **Introduction**
4
5

6 Cellular senescence is recognized as an irreversible cell cycle arrest and is induced by
7
8
9 replicative exhaustion [1] or various stresses with cellular damage [2,3]. The senescence of
10
11
12 epithelial cells has been generally thought to restrict tumour progression [4]. On the other hand,
13
14
15 the senescence of stromal cells, such as fibroblasts, has been reported to show a pro-tumourigenic
16
17
18 effect in the breast [5-7], oral cavity [8], and prostate [9], altering the secretory protein profile
19
20
21 (also called senescence-associated secretory phenotype). The senescence-associated secretory
22
23
24 proteins are various bioactive factors composed mainly of soluble signaling factors (e.g.
25
26
27 interleukins, chemokines, and growth factors), secreted proteases, or extracellular matrix (ECM)
28
29
30 components and are believed to be major factors for the cancer progression.
31
32
33

34
35 Liver cirrhosis is late-stage chronic hepatitis that is independent of the pathogenesis of
36
37
38 hepatitis, following alteration of the microenvironment with chronic inflammation. Alteration of
39
40
41 the microenvironment involves hepatic stellate cells (HSCs), the main stromal cell type in the
42
43
44 liver. HSCs become a myofibroblast-like form following various liver injuries (the formation is
45
46
47 called activation) and activated HSCs show accelerated production of secretory proteins such as
48
49
50 ECM components, cytokines, and chemokines. Continuous HSC activation alters the hepatic
51
52
53 microenvironments with excessive ECM accumulation, resulting in cirrhosis and liver failure [10].
54
55
56 In addition, senescent HSCs have also been observed in patients with liver cirrhosis, probably
57
58
59
60
61
62
63
64
65

1
2
3 derived from activated HSCs [11]. Since their discovery, senescent HSCs have been studied and
4
5
6 reported to be involved in the pathophysiology of chronic liver disorders such as cirrhosis or
7
8
9 hepatocellular carcinoma (HCC) using mouse models. However, the function of senescent HSCs
10
11
12 in HCC is not fully understood. Lujambio *et al.* reported that p53-positive senescent HSCs release
13
14
15 factors that skew macrophage polarization towards a tumour-inhibiting M1-state capable of
16
17
18 attacking senescent cells in culture [12]. In contrast, Yoshimoto *et al.* demonstrated that alterations
19
20
21 in gut microbiota induced by obesity increased the levels of deoxycholic acid provoking the
22
23
24 senescence-associated secretory phenotype in HSCs through enterohepatic circulation, resulting
25
26
27 in HCC [13]. In particular, in humans, characterization of senescent HSCs remains insufficient.
28
29
30

31
32 In the present study, we searched the gene expression profiles of senescent hHSCs for
33
34
35 senescence-associated secretory genes and investigated the gene regulation following cell
36
37
38 senescence to understand the characteristics of senescent HSCs. Thus, we identified three
39
40
41 senescence-associated secretory genes whose expression levels were up-regulated by ERK1/2
42
43
44 signalling in senescent hHSCs.
45
46
47
48
49
50
51
52
53
54
55
56
57
58
59
60
61
62
63
64
65

1
2
3 **Materials and methods**
4
5

6 *Materials*
7
8

9 Human recombinant epidermal growth factor (EGF) was obtained from PROSPEC (East
10 Brunswick, NJ, USA). SCH772984 (ERK inhibitor) was purchased from Cayman Chemical (Ann
11 Arbor, MI, USA). Primary antibodies were purchased from Cell Signaling Technology (Danvers,
12 MA, USA), Abcam (Cambridge, UK), Santa Cruz Biotechnology (Dallas, TX, USA), and
13 Millipore (Billerica, MA, USA) as shown in Table 1. Secondary antibodies for western blot
14 analysis, anti-rabbit IgG (Cat. #7074) and anti-mouse IgG (Cat. #7076), were purchased from
15 Cell Signaling Technology. The other chemicals were obtained from FUJIFILM Wako Pure
16 Chemical Corporation (Osaka, Japan) unless otherwise specified.
17
18
19
20
21
22
23
24
25
26
27
28
29
30
31
32
33
34
35
36
37

38 *Cell culture and senescence induction*
39
40

41 The human hepatic stellate cell line HHStECs (Lot #4630 and #10326 designated as “Lot 1”
42 and “Lot 2”, respectively), derived from two individuals, were purchased from ScienCell
43 Research Laboratories (Carlsbad, CA, USA). These cells were maintained using the Stellate Cell
44 Medium set (Cat. #5301) at 37 °C in a humidified 5% CO₂ atmosphere. Senescent HHStECs were
45 generated by repetitive passaging or 20 Gy of X-ray irradiation. Human dermal fibroblasts (hDFs)
46 were obtained as previously reported [14] and were maintained with DMEM at 37 °C in a 5%
47
48
49
50
51
52
53
54
55
56
57
58
59
60
61
62
63
64
65

1
2
3 CO₂ atmosphere. Senescent hDFs were generated by repetitive passaging.
4
5
6
7
8

9
10 *Doubling-time calculation and senescence-associated β-galactosidase (SA-βGal) staining*
11

12 The doubling time (DT) was evaluated by cell counting using the Cell Counter Plate (Watson,
13 Tokyo, Japan) for each cell passage. The number of cells, which were seeded initially, was 5×10⁵
14 cells/dish. DT was calculated using the following formula; $DT = T / \log_2 (P/P_0)$ [T is interval time
15 from previous passage (days); P is the number of cells at cell passage; P₀ is the number of cells
16 seeded initially]. SA-βGal positive cells were identified using the Cellular Senescence Detection
17 Kit (CELL BIOLABS, San Diego, CA, USA) according to the manufacturer's instructions.
18
19
20
21
22
23
24
25
26
27
28
29
30
31
32
33
34

35 *RNA analysis and microarray analysis*
36

37 RNA was extracted from cells using TRIzol reagent (Thermo Fisher Scientific, Waltham, MA,
38 USA) and Direct-zol RNA Miniprep (Zymo Research, Irvine, CA, USA). A gene expression array
39 was performed using the SurePrint G3 Human GE 8×60K v2 Microarray by Takara Bio Inc.
40 (Shiga, Japan). Quantitative PCR (qPCR) was performed using cDNA generated from RNA and
41 the SuperScript III Reverse Transcriptase kit (Thermo Fisher Scientific). The primers used in this
42 study are listed in Table 2. The qPCR reaction was carried out using the SYBR green PCR master
43 mix (Thermo Fisher Scientific) in the Thermal Cycler Dice Real Time System 2 (TAKARA BIO,
44
45
46
47
48
49
50
51
52
53
54
55
56
57
58
59
60
61
62
63
64
65

1
2
3 Shiga, Japan). The values were quantified using the comparative CT method and were normalized
4
5
6 to 18S ribosomal RNA. The data were expressed as the ratio to the average of the normal cell
7
8
9 group (NC) or control group.
10

11 12 13 14 15 16 *Histone extraction*

17
18
19 For western blot analysis of H2A histone family member X (H2AX) and phosphorylated H2AX
20
21
22 (γ H2AX), the protein samples were pretreated with hydrochloric acid to extract histone from cells
23
24
25 according to the histone extraction protocol provided by Abcam. Briefly, HHSteCs were washed
26
27
28 with ice-cold phosphate-buffered saline (PBS) and were suspended in the Triton extraction buffer
29
30
31 (TEB: PBS containing 0.5% (v/v) Triton X 100, 2 mM phenylmethylsulphonyl fluoride, 0.02%
32
33
34 (w/v) NaN_3). After incubation on ice for 10 min, the suspension was centrifuged (2000 rpm, 4 °C,
35
36
37 10 min). After the supernatant was discarded, the cell pellet was washed with TEB. The cell pellet
38
39
40 was suspended with 0.2 M HCl and incubated at 4 °C overnight. After centrifugation (2000 rpm,
41
42
43 4 °C, 10 min), the supernatant was subjected to western blot analysis.
44
45
46
47
48
49
50

51 *Western blot analysis*

52
53
54 Cells were homogenized with RIPA buffer (50 mM Tris-HCl at pH 7.5, 150 mM NaCl, 1% Triton
55
56
57 X-100, 1% SDS) containing the protease inhibitor cocktail cOmplete Mini (Roche, Basel,
58
59
60
61
62
63
64
65

1
2
3 Switzerland) and phosphatase inhibitors (1 mM sodium fluoride, 1 mM β -glycerol phosphate, and
4
5
6 1 mM sodium vanadate). Protein samples were subjected to 8-15% SDS-polyacrylamide gel
7
8
9 electrophoresis and were transferred to polyvinylidene difluoride membranes using standard
10
11
12 western blotting techniques. After blocking with 5% skim milk, the membranes were probed with
13
14
15 primary antibodies diluted at 1:1000 and horseradish peroxidase-conjugated secondary antibodies
16
17
18 diluted at 1:5000. Immunoreactive bands were visualized using the ImmunoStar Zeta or
19
20
21 ImmunoStar LD system and were detected using the LAS3000 or LAS4000 device (GE healthcare,
22
23
24 Chicago, IL, USA). WB Stripping Solution (Nacalai tesque, Kyoto, Japan) was used to remove
25
26
27 the antibodies from the western blot membrane.
28
29
30

31 32 33 34 35 *Flow cytometry analysis*

36
37
38 The amount of DNA per haploid was analysed using Vybrant DyeCycle Green (Thermo Fisher
39
40
41 Scientific). Diploid and tetraploid fractions were detected using the LSR II Flow Cytometer (BD
42
43
44 Biosciences, NJ, USA) after incubation with Vybrant DyeCycle Green.
45
46
47

48 49 50 51 *Immunohistochemistry*

52
53
54 HHStECs or hDFs were seeded on chamber slides (Matsunami Glass Industry Ltd, Osaka, Japan).
55
56
57 After washed with PBS containing 0.1% Tween[®] 20 (PBS-T), The cells were fixed with 4%
58
59
60

1
2
3 paraformaldehyde phosphate buffer solution (Nakalai tesque) for 1 hr at room temperature. Next,
4
5
6 the fixed cells were pre-incubated with 3% bovine serum albumin (BSA)/PBS-T for 1 hr at room
7
8
9 temperature after the cells were washed with PBS-T, and subsequently incubated with primary
10
11
12 antibody against DNA replication factor Cdt1 (CDT1) (Abcam, 1:100 dilution) or p21^{Waf1/Cip1} (Cell
13
14
15 Signaling Technology, 1:100 dilution) at 4 °C. After overnight incubation, the cells were washed
16
17
18 with PBS-T and incubated with secondary antibody AlexaFluor 594 goat anti-mouse IgG
19
20
21 (Molecular Probes, Eugene, OR, USA) for 30 min at room temperature. After adding DAPI (4',6-
22
23
24 diamidino-2-phenylindole), the cells were washed and mounted with ProLong Gold Antifade
25
26
27 Reagent (Molecular Probes, Eugene, OR, USA). The resulting cells were evaluated by BZ-X710
28
29
30 microscopy (Keyence, Osaka, Japan).
31
32
33
34
35
36
37

38 *Enzyme-linked immunosorbent assay (ELISA)*

39
40

41 Culture medium were collected after incubation with cells for 2 days. IL-8 concentration in the
42
43
44 medium was determined using the Human IL-8 ELISA MAXTM Standard Sets (BioLegend, San
45
46
47 Diego, CA).
48
49
50
51
52
53

54 *Isolation of nuclear proteins from cells*

55
56

57 Normal and senescent cells were washed twice with cold-PBS and then these nuclear and
58
59
60
61
62
63
64
65

1
2
3 cytosolic proteins of the cells were fractionated with Qproteome Cell Compartment Kit (QIAGEN,
4
5
6 Nordrhein-Westfalen, Germany). Cytosol fraction of SCs was used to check a contamination of
7
8
9 cytosolic protein in nuclear fraction.
10
11
12
13
14
15

16 *EGF stimulation*

17
18
19 HHStECs were seeded and cultured in SteCM media for 1 day. The medium was changed to
20
21
22 DMEM without foetal bovine serum for starvation (7 hr), and then EGF (diluted with 0.1% BSA)
23
24
25 was directly added to the DMEM. The BSA solution, used for the vehicle, was added to the
26
27
28 untreated group. The cells were collected after incubation for 15 min (for western blot analysis)
29
30
31 and 48 hr (for qPCR and western blot analysis).
32
33
34
35
36
37

38 *Statistical analysis*

39
40
41 Statistical analysis was performed using Prism version 6.0 software (GraphPad Software, San
42
43
44 Diego, CA, USA). A p-value of less than 0.05 was considered as a significant difference.
45
46
47
48
49
50
51
52
53
54
55
56
57
58
59
60
61
62
63
64
65

1
2
3 **Results**
4
5

6 **Generation of senescent human HSCs using repetitive passaging.**
7
8

9 HHSteCs were cultured to establish a senescent model of human HSCs. The more HHSteCs
10 were passaged, the more the doubling time increased (Fig.1A). When the passage number was
11 more than twenty, the cells showed strong senescence-associated β -galactosidase (SA- β Gal)
12 staining without enhanced mRNA levels of galactosidase beta 1 (GLB1) believed to be the origin
13 of SA- β Gal [15], and the percentage ratio of the SA- β Gal-positive cell number to the total cell
14 number was more than 70% (Fig. 1B), while that in the control cells was less than 20%. Thus,
15 more than 70% of cells represented senescent cells (SCs) and less than 20% represented normal
16 cells (NCs), respectively. In addition, SCs enhanced phosphorylated H2A histone family member
17 X protein (γ H2AX), a known DNA damage marker, and increased the protein expression level of
18 p21^{Waf1/Cip1} protein (Fig.1C), which was used as a senescence marker of HSCs in human fibrotic
19 livers [11]. Furthermore, SC increased the number of tetraploid cells without changing the number
20 of CDT1 (a specific protein for G1 phase in the cell cycle)-positive cells (Figs. 1D and 1E). Thus,
21 considering a previous report that tetraploid cells with CDT1 expression are senescent cells [16],
22 the latter was generated from HHSteCs. Using the senescent cells, we investigated the mRNA
23 levels of HSC-related genes [α -smooth muscle actin (α SMA), collagen type I alpha 1
24 (COL1A1), collagen type I alpha 2 (COL1A2), peroxisome proliferator-activated receptor gamma
25
26
27
28
29
30
31
32
33
34
35
36
37
38
39
40
41
42
43
44
45
46
47
48
49
50
51
52
53
54
55
56
57
58
59
60
61
62
63
64
65

1
2
3 (PPAR γ), and cytoglobin (CYGB)]. Unlike the gene profile of activated HSCs, the expression
4
5
6 levels of α SMA, COL1A1, COL1A2 and CYGB mRNAs were not changed in SCs, although the
7
8
9 PPAR γ mRNA levels were decreased (Fig.1F). Next, the level of interleukin (IL)-8, IL-1 β , IL-6,
10
11
12 vascular endothelial growth factor (VEGF) and serpin family E member 1 (SERPINE1), reported
13
14
15 previously as senescence-associated secretory factors, were measured. Only IL-8 mRNA levels
16
17
18 were increased in the SC (Fig.1F). Additionally enzyme-linked immunosorbent assay (ELISA)
19
20
21 indicated significantly high IL-8 concentration in the culture medium of the SCs, compared to
22
23
24 that of the NCs (Fig.1G).
25
26
27
28
29
30
31

32 **Investigation of senescence-associated secretory factors in human HSCs**

33
34

35 Microarray analysis was performed to capture senescence-associated secretory factors more
36
37
38 broadly and investigate a gene regulation of senescence-associated secretory factors in the
39
40
41 senescent HSCs. When cut-off value was 2-fold, more than 100 genes were indicated as up-
42
43
44 regulated senescence-associated secretory gene and the number was too many to perform the
45
46
47 quantitative PCR, In this study, we decided to use 4.5-fold as the cut-off value including the SAA
48
49
50 genes which were upregulated in human mesenchymal stem cells during in vitro aging [17]. From
51
52
53 the obtained results, twenty five of the highly upregulated genes in SCs were related to secretory
54
55
56 protein (Fig. 2A and Table 3). Among the 25 genes, the elevated expression of 14 genes (ANGPT1,
57
58
59
60
61
62
63
64
65

1
2
3 ANGPTL4, BMP4, CCL2, CCL7, IL-8, CYTL1, IGFBP3, PF4V1, RARRES2, SAA1, SAA2,
4
5
6 TNFRSF11B, and TNFSF15) was indicated by qPCR (Figs. 2B and 2C). Thus, we determined
7
8
9 whether the 14 genes could serve as senescence-associated secretory factors in hHSCs.
10
11
12
13
14
15

16 **Involvement of ERK1/2 in the expression of senescence-associated secretory factors in** 17 18 19 **hHSCs.** 20 21

22 The phosphorylation levels of major mitogen-activated protein kinases were measured to
23
24 understand which pathways were activated in senescent HSCs. The phosphorylation levels of
25
26 ERK1/2, but not those of JNK nor p38, were significantly increased in SCs (Figs.3A and 3B),
27
28 although MEK1/2 phosphorylation was not changed (Fig.3B). Interestingly, enhanced ERK1/2
29
30 phosphorylation was observed in nuclear fraction of the SCs (Fig.3C). Additionally, lamin B1
31
32 (LMNB1) was decreased in nucleus of SCs as previously reported [18,19]. In addition, treatment
33
34 with the ERK1/2-inhibitor SCH772984 significantly decreased the mRNA levels of ANGPTL4,
35
36 CCL7, IL-8, PF4V1, and TNFSF15 in a dose-dependent manner (0.2-, 0.3-, 0.2-, 0.6-, and 0.2-
37
38 fold at 100 nM, respectively), as shown in Fig.3D. Enhanced ERK1/2 phosphorylation was
39
40 observed when the doubling time was increased (Figs. 1A and 3E). To investigate whether
41
42 transient ERK1/2 activation induced the expression of senescence-associated secretory factors,
43
44 we tested normal HHStECs with epithelial growth factor (EGF), an activator of the ERK1/2
45
46
47
48
49
50
51
52
53
54
55
56
57
58
59
60
61
62
63
64
65

1
2
3 signalling. Transient ERK1/2 activation could not mimic the gene profile of SCs (Figs. 3F and
4
5
6 3G). Taken together, these results indicated that consecutive ERK1/2 activation leads to the
7
8
9 induction of senescence-associated secretory factor expression.
10
11
12
13
14
15

16 **Expression levels of the ERK1/2-related genes are increased in senescent human dermal**
17
18
19 **fibroblasts.**
20
21

22 To investigate whether the induction of *ANGPTL4*, *CCL7*, *IL-8*, *PF4V1* and *TNFSF15* gene
23
24
25 expression with ERK1/2 activation is specific in senescent HSCs, we generated senescent human
26
27
28 dermal fibroblasts (hDFs) by repetitive passages. Senescent hDFs exhibited obviously increased
29
30
31 SA-βGal activity, independent of *GLB1* gene expression (Fig.4A). Interestingly, senescent hDFs
32
33
34 also enhanced ERK1/2 phosphorylation (Fig.4B) and p21^{Waf1/Cip1} expression (Figs.4B and 4C) and
35
36
37 elevated the mRNA levels of *ANGPTL4*, *CCL7*, *IL-8*, *PF4V1*, and *TNFSF15* (Fig.4D). In
38
39
40
41 addition, increased concentration of IL-8 protein was clearly observed in culture medium of
42
43
44
45 senescent hDFs (Fig.4E). Taken together, the data strongly support a possibility that ERK1/2
46
47
48 activation is a common process of cell senescence in fibroblastic cells.
49
50
51
52
53

54 **Enhanced ERK1/2 phosphorylation and induction of *ANGPTL4*, *IL-8* and *PF4V1* gene**
55
56
57 **expressions were also observed in the X-ray-induced senescent HSCs.**
58
59
60
61
62
63
64
65

1
2
3 Using another model X-ray-induced cell senescence, we investigated whether ERK1/2
4
5
6 activation was enhanced and whether the mRNA levels of ANGPTL4, CCL7, IL-8, PF4V1, and
7
8
9 TNFSF15 were increased in senescent HSCs. The X-ray-induced senescent HSCs exhibited
10
11
12 obviously increased SA-βGal staining (Fig.5A). Increased p21^{Waf1/Cip1} protein levels and enhanced
13
14
15 phosphorylation of ERK1/2 were observed in X-ray-induced senescent HSCs (Fig.5B), as well as
16
17
18 in passage-induced senescent HSCs. Enhanced ERK1/2 phosphorylation appeared 24 hr after
19
20
21 exposure to X-ray irradiation, following induction of p21^{Waf1/Cip1} expression (Fig.5C). The mRNA
22
23
24 levels of ANGPTL4, IL-8 and PF4V1 were significantly increased in both of senescent Lot1 and
25
26
27 Lot2 cells, while those of CCL7 and TNFSF15 mRNA were increased in Lot2 cells but not in
28
29
30 Lot1 cells (Fig.5D). These senescent cells showed elevated concentration of IL-8 protein in the
31
32
33 culture medium as well as the passage-induced senescent cells (Fig.5E). These results may
34
35
36 indicate that the simultaneous event of *ANGPTL4*, *IL-8*, and *PF4V1* gene induction by ERK1/2
37
38
39 activation is a common phenomenon in senescent hHSCs.
40
41
42
43
44
45
46
47
48
49
50
51
52
53
54
55
56
57
58
59
60
61
62
63
64
65

1
2
3 **Discussion**
4

5 The current study investigated the gene expression profile of senescent human HSCs *in vitro*,
6
7
8 utilizing senescent HSC models derived from HHSteCs, and demonstrated that ERK1/2
9
10 phosphorylation was enhanced in senescent hHSCs and was involved in the expressions of
11
12 *ANGPTL4*, *IL-8* and *PF4V1* genes. Interestingly, enhanced ERK1/2 phosphorylation and induced
13
14 *ANGPTL4*, *IL-8* and *PF4V1* expressions were not only observed in passage-induced senescent
15
16
17
18 hHSCs but also in X ray-induced senescent hHSCs and senescent hDFs.
19
20
21
22

23
24 Our results suggest that ERK1/2 activation is a common senescence-associated factor in
25
26 fibroblastic cells and is involved in the gene regulation of senescence-associated secretory factors
27
28 (ANGPTL4, IL-8 and PF4V1). Phosphorylated ERK1/2 was increased in nucleus of senescent
29
30 HSCs, which strongly supports that ERK1/2 activation plays a role of senescence-associated gene
31
32 regulation in the HSCs. However, transient ERK1/2 activation (EGF treatment) could not fully
33
34 mimic the gene expression profile of senescent HSCs in normal HSCs. These results may indicate
35
36 a requirement of continuous ERK1/2 activation or involvement of other senescence-associated
37
38 factors in gene regulation. Reduced activities of protein phosphatases 1 and 2A was reported to
39
40 be involved in senescence-associated activation of ERK1/2 in normal human diploid fibroblasts
41
42 [20]. Decreased activities of the phosphatases may be important to elevate ERK1/2
43
44 phosphorylation in the senescent HSCs. Senescence-associated secretory factors have been
45
46 demonstrated to be regulated by NF- κ B [21], CCAAT/enhancer-binding protein beta [22], p38
47
48
49
50
51
52
53
54
55
56
57
58
59
60
61
62
63
64
65

1
2
3 [23], and mammalian target of rapamycin signaling [24,25]. Further study of the interaction
4
5
6 between ERK1/2 and these factors is also needed to fully understand the related regulatory
7
8
9 mechanisms.
10

11
12 ANGPTL4, IL-8, and PF4V1 have been reported to be associated with the progression of
13
14 various cancers. For example, ANGPTL4 is a factor involved in the progression of human
15
16 colorectal cancer, especially venous invasion and distant metastasis [26]. Increased expression of
17
18 IL-8 in the tumour microenvironment enhanced the growth and metastasis of colon cancer [27].
19
20 In addition, endogenous PF4V1 (also known as CXCL4L1) promoted the growth of pancreatic
21
22 ductal adenocarcinoma (Panc-1 cells), independently of its anti-angiogenic function [28].
23
24 Furthermore, IL-8 and ANGPTL4 are also known to accelerate the progression of HCC; Zhu *et*
25
26 *al.* demonstrated that activated HSCs within the stroma of HCC contributed to tumour
27
28 angiogenesis via IL-8 [29]; Li *et al.* suggested that ANGPTL4 could significantly promote HCC
29
30 cell invasion and metastasis *in vitro* and *in vivo* [30]. Taken together, these observations and the
31
32 current study suggest that senescent HSCs affect the microenvironment surrounding HCC through
33
34 the secretion of ANGPTL4, IL-8 and PF4V1. In this study, the induction of these genes was
35
36 regulated by ERK1/2 in the senescent HSCs. Sorafenib, a multiple receptor tyrosine kinase
37
38 inhibitor that also targets ERK1/2, is a recommended drug for advanced HCC. Sorafenib was
39
40 shown to directly act on HSCs in rats and attenuate liver fibrosis by reducing HSC proliferation
41
42
43
44
45
46
47
48
49
50
51
52
53
54
55
56
57
58
59
60
61
62
63
64
65

1
2
3 [31]. Sorafenib might exert its therapeutic effect by suppressing senescent HSCs with enhanced
4
5
6 ERK1/2 activation, leading to the alleviation of HCC.
7
8

9 Boosting specific immune cell populations may be effective in controlling senescent HSCs,
10
11 because natural killer cells have been suggested to selectively kill senescent HSCs [11]. However,
12
13 many issues remain to be solved to understand the importance of senescent HSCs in human liver
14
15 disease including HCC; 1) A specific marker of senescent HSCs is currently lacking; 2)
16
17 Qualitative and quantitative information on senescence-associated secretory factors have been
18
19 limited in patients. Future studies are vitally required to establish a concept of the manipulation
20
21 of senescent HSCs to cure liver cancers.
22
23
24
25
26
27
28
29
30

31 In conclusion, we identified senescence-associated secretory factors regulated by ERK1/2
32
33 pathways that were also activated in senescent hHSCs and hDFs. These results revealed a novel
34
35 role of ERK1/2 in hHSCs, suggesting that the simultaneous induction of *ANGPTL4*, *IL-8*, and
36
37 *PF4VI* gene can serve as a cell senescence marker in hHSCs. This study may provide a clue about
38
39 the pathophysiological roles of senescent HSCs in HCC and the possibility of therapeutic
40
41 targeting of senescent HSCs.
42
43
44
45
46
47
48
49
50
51
52
53
54
55
56
57
58
59
60
61
62
63
64
65

1
2
3 **Acknowledgments**
4
5

6 We thank Atsuko Daikoku (Osaka City University), Kenji Kitamura (Osaka City
7
8
9
10 University) and Junko Kawawaki (Research support platform of Osaka City University
11
12
13 Graduate School of Medicine) for technical assistance.
14
15
16
17
18

19 **Grants**
20
21

22 This work was supported by The Uehara Memorial Foundation, The Osaka Medical
23
24
25 Research Foundation for Intractable Diseases, The Tokyo Biochemical Research Foundation,
26
27
28 The Osaka City University Strategic Research Grant 2016 for young researchers, JSPS
29
30
31 KAKENHI Grant Number JP26870501 and JP17K18012, and a Grant for Research Program
32
33
34 on Hepatitis from the Japan Agency for Medical Research and Development (AMED) Grant
35
36
37
38 Number 16fk0210104h0001.
39
40
41
42
43

44 **Disclosures**
45
46

47 No conflicts of interest, financial or otherwise, are declared by the authors
48
49
50
51
52
53

54 **Author contributions**
55
56
57
58
59
60
61
62
63
64
65

1
2
3
4
5
6
7
8
9
10
11
12
13
14
15
16
17
18
19
20
21
22
23
24
25
26
27
28
29
30
31
32
33
34
35
36
37
38
39
40
41
42
43
44
45
46
47
48
49
50
51
52
53
54
55
56
57
58
59
60
61
62
63
64
65

N.O. and T.M. designed the experiments and interpreted the results. N.O., T.M., M.H., S.T.,
H.U., M.S.M., and Y. T. conducted the experiments and prepared the figures. N.O., T.M., K.Y.,
N.K., and K.I. wrote and revised the manuscript.

1
2
3 **Figure legends**
4
5

6 **Figure 1. Generation of senescent HSCs by replicative passaging.**
7
8

9 (A) Calculated doubling time of HHSteCs at passages 5, 17, and 27. (B) Expression of
10 senescence-associated β -galactosidase (SA- β Gal). Normal cells (NCs) and senescent cells (SCs)
11 represent HHSteCs at passages 10 and 31, respectively. These cells were stained using the SA-
12 β Gal staining kit (left). Bold bars represent 200 μ m. SA- β Gal-positive cells were counted and the
13 value was calculated as the percentage ratio of SA- β Gal-positive cells to the total cells. The data
14 are expressed as means of four individual fields (centre). qPCR analysis of galactosidase beta 1
15 (GLB1) mRNA (right). The data are expressed as means and SD (n = 3). (C) Western blot analysis
16 of phosphorylated H2A histone family member X (γ H2AX) and p21^{Waf1/Cip1} proteins. Total H2AX
17 and glyceraldehyde-3-phosphate dehydrogenase (GAPDH) were used as loading controls,
18 respectively. (D) Flow cytometry analysis of the DNA amounts using Vybrant[®] DyeCycle[™]
19 Green. The percentage ratios of diploid (2N) and tetraploid (4N) cells to total cells are indicated
20 in the figure. (E) Immunofluorescence staining analysis of CDT1 proteins (red). 4',6-Diamidino-
21 2-phenylindole (DAPI) was used for nuclear counterstaining. The yellow bars represent 100 μ m
22 in the photos. (F) qPCR analysis of the mRNA expressions of HSCs-related genes (left) and
23 senescence-associated secretory phenotype-related genes (right). The data are expressed as means
24 and SD (n=3-4). Significance was determined by unpaired t test (*, P<0.05). (G) IL-8 protein
25
26
27
28
29
30
31
32
33
34
35
36
37
38
39
40
41
42
43
44
45
46
47
48
49
50
51
52
53
54
55
56
57
58
59
60
61
62
63
64
65

1
2
3 concentrations in culture medium. The data are expressed as means and SD (n=3). Significance
4
5
6 was determined by unpaired t test (*, P<0.05).
7
8
9

10
11
12 **Figure 2. Gene expression analysis of secretory genes in SCs.**
13
14

15
16 (A) Microarray gene expression analysis. Twenty-five genes encoding secretory proteins were
17
18 identified as up-regulated genes in SCs (4.5-fold increase). (B and C) qPCR analysis of the
19
20 secretory gene expressions in the SCs of Lot 1 and Lot 2. The column and bar represent mean and
21
22 SD, respectively (n=3-5). Significant increased values greater than 2-fold are summarized in the
23
24
25
26
27
28
29 C panel. Significance was determined by unpaired Student t-test (P<0.05).
30
31
32
33
34

35 **Figure 3. ERK1/2 signalling is involved in the regulation of senescence-associated secretory**
36

37
38 **factors in HSCs.** (A) Western blot analysis of major mitogen-activated protein kinase pathways
39
40 in the SCs of HHStcC. (B) Western blot analysis of ERK1/2 and MEK1/2 phosphorylations.
41
42 ERK1/2 phosphorylation levels were quantified. The signal intensity was measured using image
43
44
45
46
47
48
49
50
51
52
53
54
55
56
57
58
59
60
61
62
63
64
65
66
67
68
69
70
71
72
73
74
75
76
77
78
79
80
81
82
83
84
85
86
87
88
89
90
91
92
93
94
95
96
97
98
99
100
101
102
103
104
105
106
107
108
109
110
111
112
113
114
115
116
117
118
119
120
121
122
123
124
125
126
127
128
129
130
131
132
133
134
135
136
137
138
139
140
141
142
143
144
145
146
147
148
149
150
151
152
153
154
155
156
157
158
159
160
161
162
163
164
165
166
167
168
169
170
171
172
173
174
175
176
177
178
179
180
181
182
183
184
185
186
187
188
189
190
191
192
193
194
195
196
197
198
199
200
201
202
203
204
205
206
207
208
209
210
211
212
213
214
215
216
217
218
219
220
221
222
223
224
225
226
227
228
229
230
231
232
233
234
235
236
237
238
239
240
241
242
243
244
245
246
247
248
249
250
251
252
253
254
255
256
257
258
259
260
261
262
263
264
265
266
267
268
269
270
271
272
273
274
275
276
277
278
279
280
281
282
283
284
285
286
287
288
289
290
291
292
293
294
295
296
297
298
299
300
301
302
303
304
305
306
307
308
309
310
311
312
313
314
315
316
317
318
319
320
321
322
323
324
325
326
327
328
329
330
331
332
333
334
335
336
337
338
339
340
341
342
343
344
345
346
347
348
349
350
351
352
353
354
355
356
357
358
359
360
361
362
363
364
365
366
367
368
369
370
371
372
373
374
375
376
377
378
379
380
381
382
383
384
385
386
387
388
389
390
391
392
393
394
395
396
397
398
399
400
401
402
403
404
405
406
407
408
409
410
411
412
413
414
415
416
417
418
419
420
421
422
423
424
425
426
427
428
429
430
431
432
433
434
435
436
437
438
439
440
441
442
443
444
445
446
447
448
449
450
451
452
453
454
455
456
457
458
459
460
461
462
463
464
465
466
467
468
469
470
471
472
473
474
475
476
477
478
479
480
481
482
483
484
485
486
487
488
489
490
491
492
493
494
495
496
497
498
499
500
501
502
503
504
505
506
507
508
509
510
511
512
513
514
515
516
517
518
519
520
521
522
523
524
525
526
527
528
529
530
531
532
533
534
535
536
537
538
539
540
541
542
543
544
545
546
547
548
549
550
551
552
553
554
555
556
557
558
559
560
561
562
563
564
565
566
567
568
569
570
571
572
573
574
575
576
577
578
579
580
581
582
583
584
585
586
587
588
589
590
591
592
593
594
595
596
597
598
599
600
601
602
603
604
605
606
607
608
609
610
611
612
613
614
615
616
617
618
619
620
621
622
623
624
625
626
627
628
629
630
631
632
633
634
635
636
637
638
639
640
641
642
643
644
645
646
647
648
649
650
651
652
653
654
655
656
657
658
659
660
661
662
663
664
665
666
667
668
669
670
671
672
673
674
675
676
677
678
679
680
681
682
683
684
685
686
687
688
689
690
691
692
693
694
695
696
697
698
699
700
701
702
703
704
705
706
707
708
709
710
711
712
713
714
715
716
717
718
719
720
721
722
723
724
725
726
727
728
729
730
731
732
733
734
735
736
737
738
739
740
741
742
743
744
745
746
747
748
749
750
751
752
753
754
755
756
757
758
759
760
761
762
763
764
765
766
767
768
769
770
771
772
773
774
775
776
777
778
779
780
781
782
783
784
785
786
787
788
789
790
791
792
793
794
795
796
797
798
799
800
801
802
803
804
805
806
807
808
809
810
811
812
813
814
815
816
817
818
819
820
821
822
823
824
825
826
827
828
829
830
831
832
833
834
835
836
837
838
839
840
841
842
843
844
845
846
847
848
849
850
851
852
853
854
855
856
857
858
859
860
861
862
863
864
865
866
867
868
869
870
871
872
873
874
875
876
877
878
879
880
881
882
883
884
885
886
887
888
889
890
891
892
893
894
895
896
897
898
899
900
901
902
903
904
905
906
907
908
909
910
911
912
913
914
915
916
917
918
919
920
921
922
923
924
925
926
927
928
929
930
931
932
933
934
935
936
937
938
939
940
941
942
943
944
945
946
947
948
949
950
951
952
953
954
955
956
957
958
959
960
961
962
963
964
965
966
967
968
969
970
971
972
973
974
975
976
977
978
979
980
981
982
983
984
985
986
987
988
989
990
991
992
993
994
995
996
997
998
999
1000

1
2
3 cytosolic proteins in nuclear fraction. Lamin B1 (LMNB1) and GAPDH were used as loading
4
5
6 control of nuclear and cytosol fractions, respectively. (D) Effect of treatment with SCH772984
7
8
9 on the expression of senescence-associated secretory genes in SCs. The column and bar represent
10
11
12 mean and SD, respectively (n=3). Significance was determined by one-way ANOVA with
13
14
15 Dunnett's test (*, P<0.05). (E) Change in the phosphorylated ERK1/2 levels of HHSteCs after
16
17
18 replicative passaging. 5, 17 and 27 indicate the passage number. (F) Western blot analysis of
19
20
21 ERK1/2 phosphorylation after treatment with human EGF. (G) qPCR analysis of ANGPTL4,
22
23
24 CCL7, IL-8, PF4V1 and TNFSF15 mRNAs after EGF treatment. The column and bar represent
25
26
27 mean and SD, respectively (n=3). Significance was determined by one-way ANOVA with
28
29
30 Dunnett's test (*, P<0.05).
31
32
33
34
35
36
37

38 **Figure.4. Enhancement of ERK1/2 phosphorylation and induction of ERK-related gene**
39
40
41 **expression were observed in the senescent human DFs (hDFs).**
42

43
44 (A) Expression of SA-βGal in hDFs at passage 7 (NC) and 26 (SC). These cells were stained
45
46 using the SA-βGal staining kit (left). Bold bars represent 200 μm. SA-βGal-positive cells were
47
48 counted and the value were calculated as percentage ratios of SA-βGal-positive cells to total cells.
49
50
51 The data are expressed as means from four individual fields (centre). qPCR analysis of GLB1
52
53
54 mRNA (right). The data are expressed as means and SD (n=3). (B) Western blot analysis of
55
56
57
58
59
60
61
62
63
64
65

1
2
3 p21^{Waf1/Cip1} and ERK1/2 phosphorylation in senescent hDFs. GAPDH was used as a loading
4
5
6 control. (C) Immunofluorescence staining analysis of p21^{Waf1/Cip1} proteins (green). DAPI was used
7
8
9 for nuclear counterstaining. The yellow bars represent 50 μ m in the photos. (D) qPCR analysis of
10
11
12 secretory factor mRNAs enhanced in senescent HSCs. The column and bar represent mean and
13
14
15 SD, respectively (n=3). Significance was determined by unpaired Student t-test (*, P<0.05). (E)
16
17
18 IL-8 protein concentrations in the culture medium. The column and bar represent mean and SD,
19
20
21 respectively (n=3). Significance was determined by unpaired Student t-test (*, P<0.05).
22
23
24
25
26
27
28

29 **Figure 5. Enhancement of ERK1/2 phosphorylation and induction of ANGPTL4, IL-8, and**
30 **PF4V1 gene expression are observed in X-ray-induced senescent HSCs.**
31

32
33
34
35 (A) Expression of SA- β Gal after exposure to X ray-irradiation. X-SC and X-NC were donated as
36
37
38 the X-ray-exposure group and control group, respectively. These cells were stained using the SA-
39
40
41 β Gal staining kit (left). Bold bars represent 200 μ m. SA- β Gal-positive cells were counted and the
42
43
44 values were calculated as percentage ratios of SA- β Gal-positive cells to total cells. The data are
45
46
47 expressed as means from four individual fields (centre). qPCR analysis of GLB1 mRNA (right).
48
49
50
51 The data are expressed as means and SD (n=3). (B) Western blot analysis of ERK1/2
52
53
54 phosphorylation and p21^{Waf1/Cip1} in the X-SC group. (C) Sequential analysis of ERK1/2
55
56
57 phosphorylation and p21^{Waf1/Cip1} expression in HHStECs after X-ray irradiation. GAPDH was used
58
59
60
61
62
63
64
65

1
2
3 as a loading control in western blot analysis. (D) qPCR analysis of ERK1/2-related genes revealed
4
5
6 in senescent HSCs. Two individual lots of HHSteCs (Lot 1 and Lot 2) were used for analysis. The
7
8
9 column and bar represent mean and SD, respectively (n=3). Significance was determined by
10
11
12 unpaired Student's t-test (*, P<0.05). (E) IL-8 protein concentrations in the culture medium. The
13
14
15 column represents average of triplicate values in one experiment.
16
17
18
19
20
21
22
23
24
25
26
27
28
29
30
31
32
33
34
35
36
37
38
39
40
41
42
43
44
45
46
47
48
49
50
51
52
53
54
55
56
57
58
59
60
61
62
63
64
65

References

1. Hayflick L, Moorhead PS (1961) The serial cultivation of human diploid cell strains. *Exp Cell Res* 25:585-621
2. Campisi J, d'Adda di Fagagna F (2007) Cellular senescence: when bad things happen to good cells. *Nat Rev Mol Cell Biol* 8 (9):729-740. doi:10.1038/nrm2233
3. Serrano M, Lin AW, McCurrach ME, Beach D, Lowe SW (1997) Oncogenic ras provokes premature cell senescence associated with accumulation of p53 and p16INK4a. *Cell* 88 (5):593-602
4. Collado M, Blasco MA, Serrano M (2007) Cellular senescence in cancer and aging. *Cell* 130 (2):223-233. doi:10.1016/j.cell.2007.07.003
5. Parrinello S, Coppe JP, Krtolica A, Campisi J (2005) Stromal-epithelial interactions in aging and cancer: senescent fibroblasts alter epithelial cell differentiation. *J Cell Sci* 118 (Pt 3):485-496. doi:10.1242/jcs.01635
6. Krtolica A, Parrinello S, Lockett S, Desprez PY, Campisi J (2001) Senescent fibroblasts promote epithelial cell growth and tumorigenesis: a link between cancer and aging. *Proc Natl Acad Sci U S A* 98 (21):12072-12077. doi:10.1073/pnas.211053698
7. Liu D, Hornsby PJ (2007) Senescent human fibroblasts increase the early growth of xenograft tumors via matrix metalloproteinase secretion. *Cancer Res* 67 (7):3117-3126. doi:10.1158/0008-5472.CAN-06-3452
8. Coppe JP, Boisen M, Sun CH, Wong BJ, Kang MK, Park NH, Desprez PY, Campisi J, Krtolica A (2008) A role for fibroblasts in mediating the effects of tobacco-induced epithelial cell growth and invasion. *Mol Cancer Res* 6 (7):1085-1098. doi:10.1158/1541-7786.MCR-08-0062
9. Bavik C, Coleman I, Dean JP, Knudsen B, Plymate S, Nelson PS (2006) The gene expression program of prostate fibroblast senescence modulates neoplastic epithelial cell proliferation through paracrine mechanisms. *Cancer Res* 66 (2):794-802. doi:10.1158/0008-5472.CAN-05-1716
10. Tsuchida T, Friedman SL (2017) Mechanisms of hepatic stellate cell activation. *Nat Rev Gastroenterol Hepatol* 14 (7):397-411. doi:10.1038/nrgastro.2017.38
11. Krizhanovsky V, Yon M, Dickins RA, Hearn S, Simon J, Miething C, Yee H, Zender L, Lowe SW (2008) Senescence of activated stellate cells limits liver fibrosis. *Cell* 134 (4):657-667. doi:10.1016/j.cell.2008.06.049
12. Lujambio A, Akkari L, Simon J, Grace D, Tschaharganeh DF, Bolden JE, Zhao Z, Thapar V, Joyce JA, Krizhanovsky V, Lowe SW (2013) Non-cell-autonomous tumor suppression by p53. *Cell* 153 (2):449-460. doi:10.1016/j.cell.2013.03.020

- 1
2
3 13. Yoshimoto S, Loo TM, Atarashi K, Kanda H, Sato S, Oyadomari S, Iwakura Y, Oshima K,
4 Morita H, Hattori M, Honda K, Ishikawa Y, Hara E, Ohtani N (2013) Obesity-induced gut
5 microbial metabolite promotes liver cancer through senescence secretome. *Nature* 499
6 (7456):97-101. doi:10.1038/nature12347
7
8 14. Saito N, Adachi H, Tanaka H, Nakata S, Kawada N, Oofusa K, Yoshizato K (2017)
9 Interstitial fluid flow-induced growth potential and hyaluronan synthesis of fibroblasts in a
10 fibroblast-populated stretched collagen gel culture. *Biochim Biophys Acta* 1861 (9):2261-2273.
11 doi:10.1016/j.bbagen.2017.06.019
12
13 15. Lee BY, Han JA, Im JS, Morrone A, Johung K, Goodwin EC, Kleijer WJ, DiMaio D, Hwang
14 ES (2006) Senescence-associated beta-galactosidase is lysosomal beta-galactosidase. *Aging*
15 *Cell* 5 (2):187-195. doi:10.1111/j.1474-9726.2006.00199.x
16
17 16. Johmura Y, Shimada M, Misaki T, Naiki-Ito A, Miyoshi H, Motoyama N, Ohtani N, Hara
18 E, Nakamura M, Morita A, Takahashi S, Nakanishi M (2014) Necessary and sufficient role
19 for a mitosis skip in senescence induction. *Mol Cell* 55 (1):73-84.
20 doi:10.1016/j.molcel.2014.05.003
21
22 17. Ebert R, Benisch P, Krug M, Zeck S, Meissner-Weigl J, Steinert A, Rauner M, Hofbauer
23 L, Jakob F (2015) Acute phase serum amyloid A induces proinflammatory cytokines and
24 mineralization via toll-like receptor 4 in mesenchymal stem cells. *Stem Cell Res* 15 (1):231-
25 239. doi:10.1016/j.scr.2015.06.008
26
27 18. Freund A, Laberge RM, Demaria M, Campisi J (2012) Lamin B1 loss is a senescence-
28 associated biomarker. *Mol Biol Cell* 23 (11):2066-2075. doi:10.1091/mbc.E11-10-0884
29
30 19. Shimi T, Butin-Israeli V, Adam SA, Hamanaka RB, Goldman AE, Lucas CA, Shumaker
31 DK, Kosak ST, Chandel NS, Goldman RD (2011) The role of nuclear lamin B1 in cell
32 proliferation and senescence. *Genes Dev* 25 (24):2579-2593. doi:10.1101/gad.179515.111
33
34 20. Kim HS, Song MC, Kwak IH, Park TJ, Lim IK (2003) Constitutive induction of p-Erk1/2
35 accompanied by reduced activities of protein phosphatases 1 and 2A and MKP3 due to
36 reactive oxygen species during cellular senescence. *J Biol Chem* 278 (39):37497-37510.
37 doi:10.1074/jbc.M211739200
38
39 21. Chien Y, Scuoppo C, Wang X, Fang X, Balgley B, Bolden JE, Premsrirut P, Luo W, Chicas
40 A, Lee CS, Kogan SC, Lowe SW (2011) Control of the senescence-associated secretory
41 phenotype by NF-kappaB promotes senescence and enhances chemosensitivity. *Genes Dev*
42 25 (20):2125-2136. doi:10.1101/gad.17276711
43
44 22. Kuilman T, Michaloglou C, Vredeveld LC, Douma S, van Doorn R, Desmet CJ, Aarden LA,
45 Mooi WJ, Peeper DS (2008) Oncogene-induced senescence relayed by an interleukin-
46 dependent inflammatory network. *Cell* 133 (6):1019-1031. doi:10.1016/j.cell.2008.03.039
47
48 23. Freund A, Patil CK, Campisi J (2011) p38MAPK is a novel DNA damage response-
49
50
51
52
53
54
55
56
57
58
59
60
61
62
63
64
65

1
2 independent regulator of the senescence-associated secretory phenotype. *EMBO J* 30
3 (8):1536-1548. doi:10.1038/emboj.2011.69

4
5 24. Herranz N, Gallage S, Mellone M, Wuestefeld T, Klotz S, Hanley CJ, Raguz S, Acosta JC,
6 Innes AJ, Banito A, Georgilis A, Montoya A, Wolter K, Dharmalingam G, Faull P, Carroll T,
7 Martinez-Barbera JP, Cutillas P, Reisinger F, Heikenwalder M, Miller RA, Withers D, Zender
8 L, Thomas GJ, Gil J (2015) mTOR regulates MAPKAPK2 translation to control the
9 senescence-associated secretory phenotype. *Nat Cell Biol* 17 (9):1205-1217.
10 doi:10.1038/ncb3225

11
12 25. Laberge RM, Sun Y, Orjalo AV, Patil CK, Freund A, Zhou L, Curran SC, Davalos AR,
13 Wilson-Edell KA, Liu S, Limbad C, Demaria M, Li P, Hubbard GB, Ikeno Y, Javors M,
14 Desprez PY, Benz CC, Kapahi P, Nelson PS, Campisi J (2015) MTOR regulates the pro-
15 tumorigenic senescence-associated secretory phenotype by promoting IL1A translation. *Nat*
16 *Cell Biol* 17 (8):1049-1061. doi:10.1038/ncb3195

17
18 26. Nakayama T, Hirakawa H, Shibata K, Nazneen A, Abe K, Nagayasu T, Taguchi T (2011)
19 Expression of angiopoietin-like 4 (ANGPTL4) in human colorectal cancer: ANGPTL4
20 promotes venous invasion and distant metastasis. *Oncol Rep* 25 (4):929-935.
21 doi:10.3892/or.2011.1176

22
23 27. Lee YS, Choi I, Ning Y, Kim NY, Khatchadourian V, Yang D, Chung HK, Choi D, LaBonte
24 MJ, Ladner RD, Nagulapalli Venkata KC, Rosenberg DO, Petasis NA, Lenz HJ, Hong YK
25 (2012) Interleukin-8 and its receptor CXCR2 in the tumour microenvironment promote colon
26 cancer growth, progression and metastasis. *Br J Cancer* 106 (11):1833-1841.
27 doi:10.1038/bjc.2012.177

28
29 28. Quemener C, Baud J, Boye K, Dubrac A, Billottet C, Soulet F, Darlot F, Dumartin L, Sire
30 M, Grepin R, Daubon T, Rayne F, Wodrich H, Couvelard A, Pineau R, Schilling M, Castronovo
31 V, Sue SC, Clarke K, Lomri A, Khatib AM, Hagedorn M, Prats H, Bikfalvi A (2016) Dual
32 Roles for CXCL4 Chemokines and CXCR3 in Angiogenesis and Invasion of Pancreatic Cancer.
33 *Cancer Res* 76 (22):6507-6519. doi:10.1158/0008-5472.CAN-15-2864

34
35 29. Zhu B, Lin N, Zhang M, Zhu Y, Cheng H, Chen S, Ling Y, Pan W, Xu R (2015) Activated
36 hepatic stellate cells promote angiogenesis via interleukin-8 in hepatocellular carcinoma. *J*
37 *Transl Med* 13:365. doi:10.1186/s12967-015-0730-7

38
39 30. Li H, Ge C, Zhao F, Yan M, Hu C, Jia D, Tian H, Zhu M, Chen T, Jiang G, Xie H, Cui Y,
40 Gu J, Tu H, He X, Yao M, Liu Y, Li J (2011) Hypoxia-inducible factor 1 alpha-activated
41 angiopoietin-like protein 4 contributes to tumor metastasis via vascular cell adhesion
42 molecule-1/integrin beta1 signaling in human hepatocellular carcinoma. *Hepatology* 54
43 (3):910-919. doi:10.1002/hep.24479

44
45 31. Wang Y, Gao J, Zhang D, Zhang J, Ma J, Jiang H (2010) New insights into the antifibrotic
46
47
48
49
50
51
52
53
54
55
56
57
58
59
60
61
62
63
64
65

1
2
3
4
5
6
7
8
9
10
11
12
13
14
15
16
17
18
19
20
21
22
23
24
25
26
27
28
29
30
31
32
33
34
35
36
37
38
39
40
41
42
43
44
45
46
47
48
49
50
51
52
53
54
55
56
57
58
59
60
61
62
63
64
65

effects of sorafenib on hepatic stellate cells and liver fibrosis. *J Hepatol* 53 (1):132-144.
doi:10.1016/j.jhep.2010.02.027

Figure 1

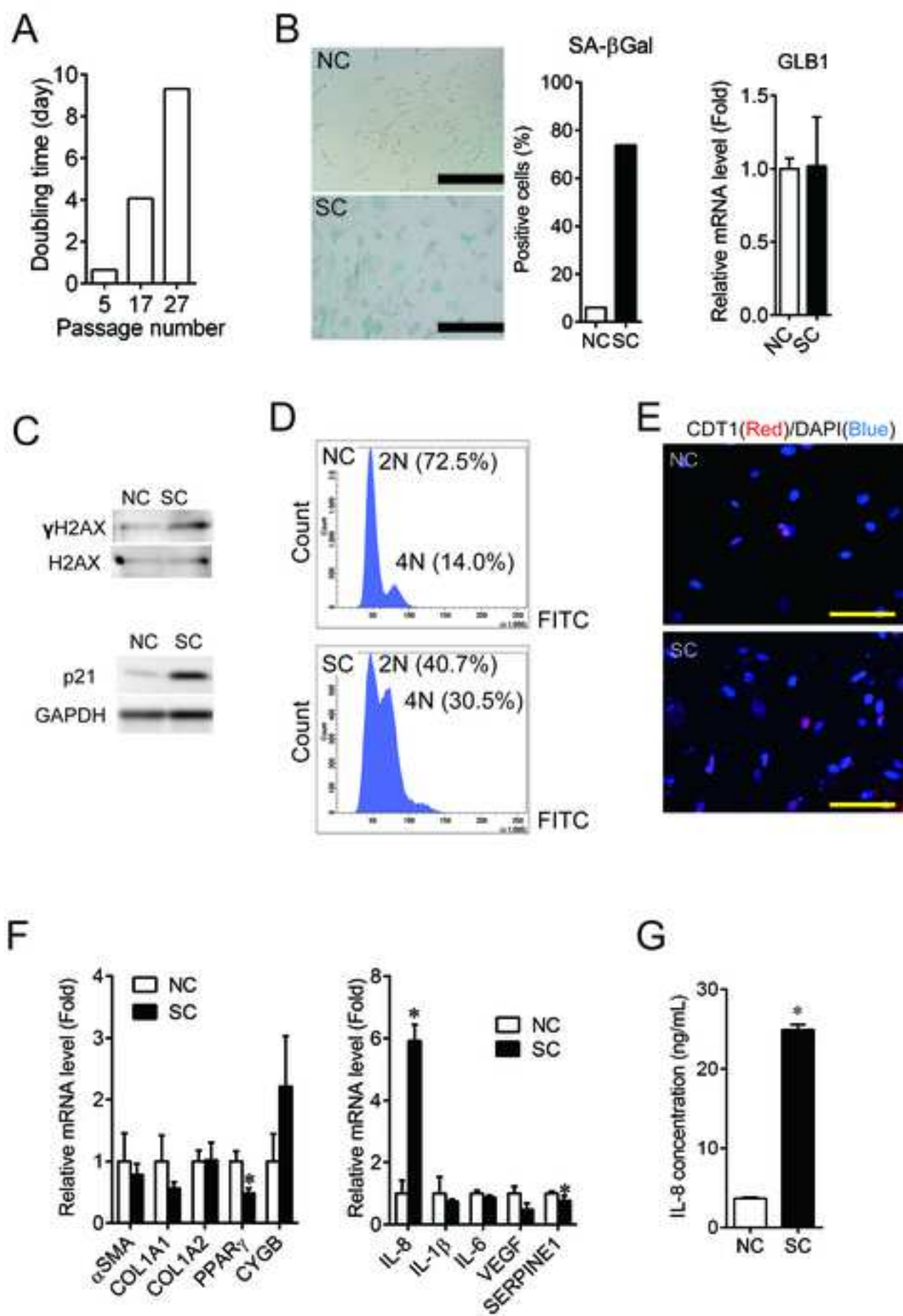


Figure 2

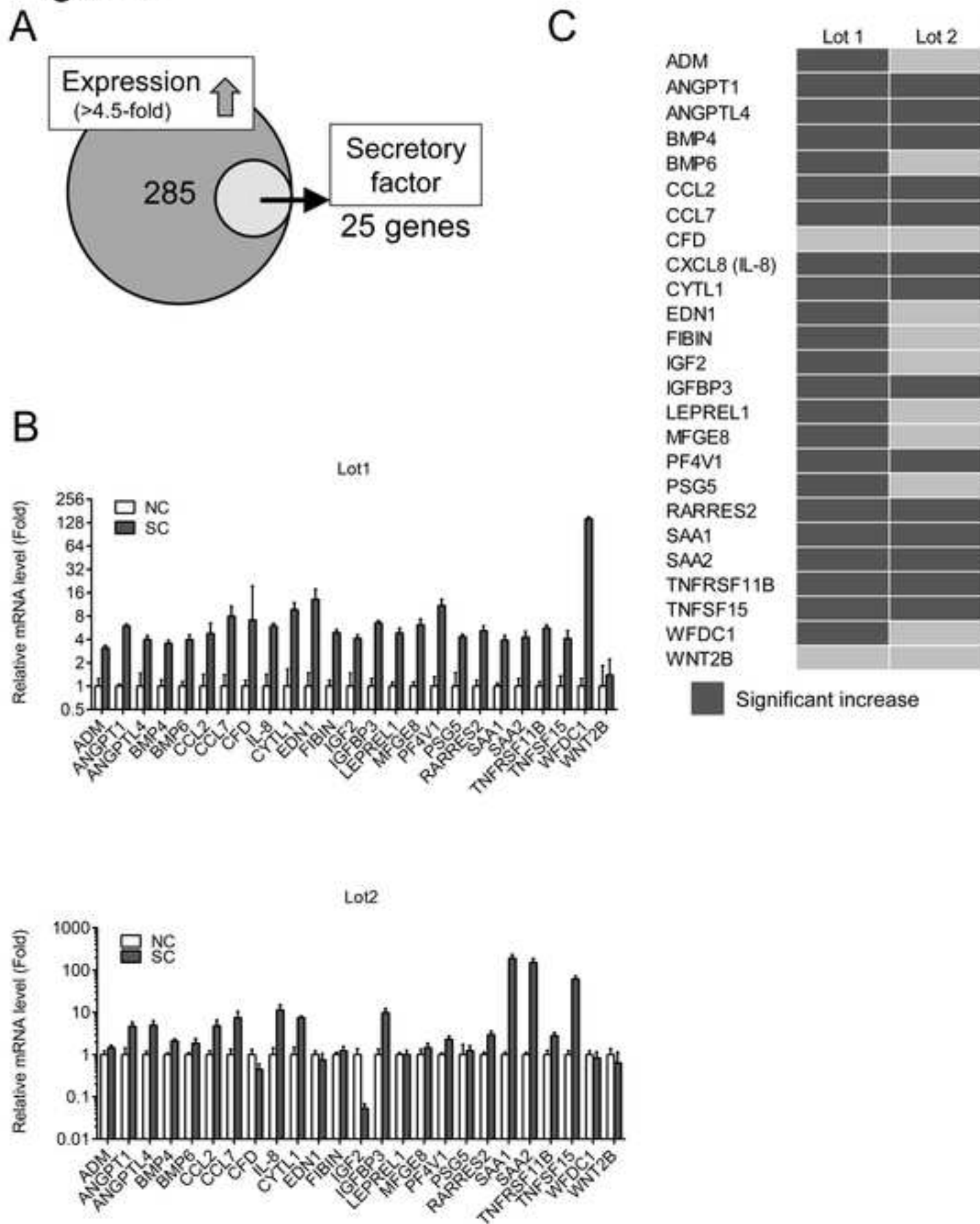


Figure 3

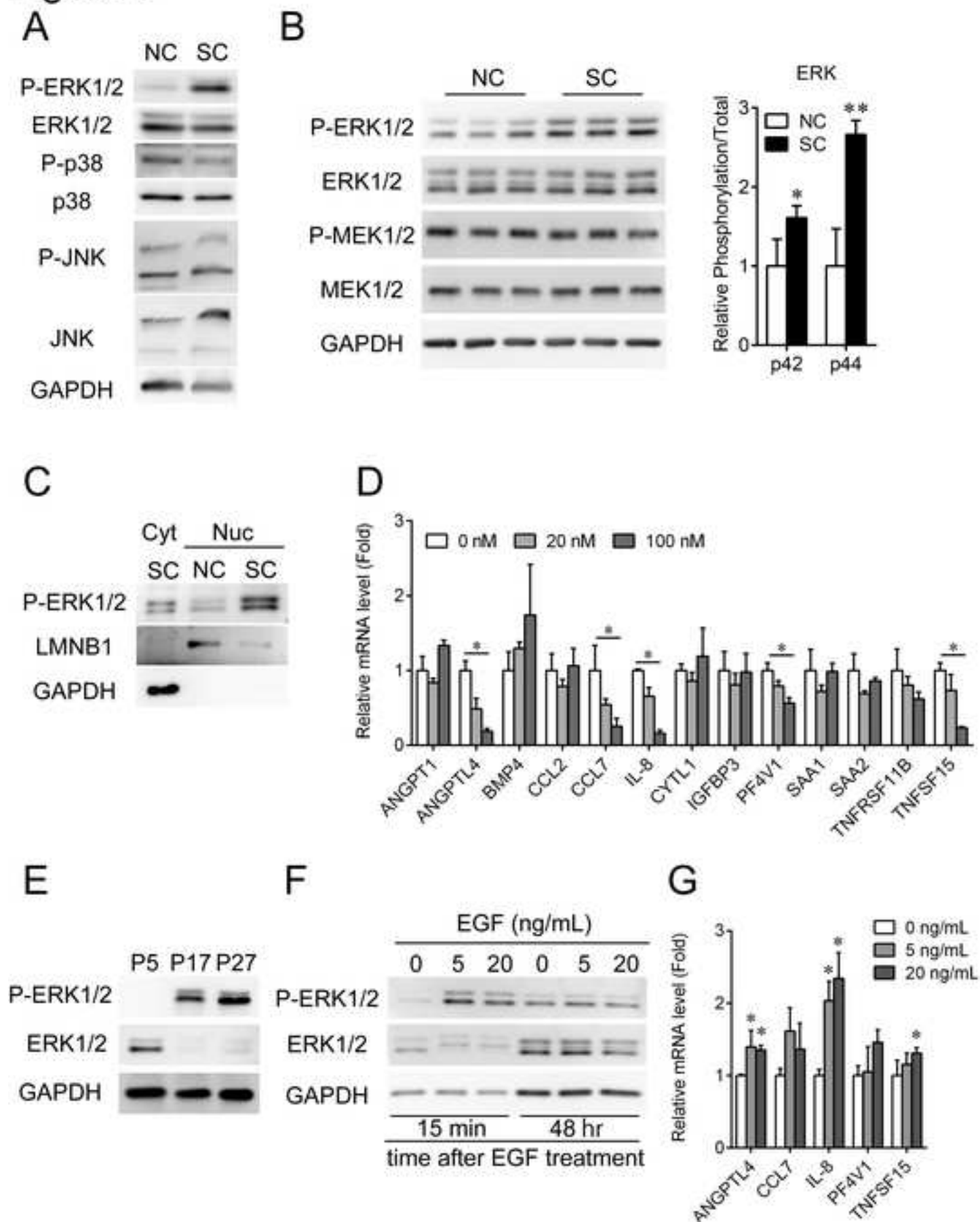
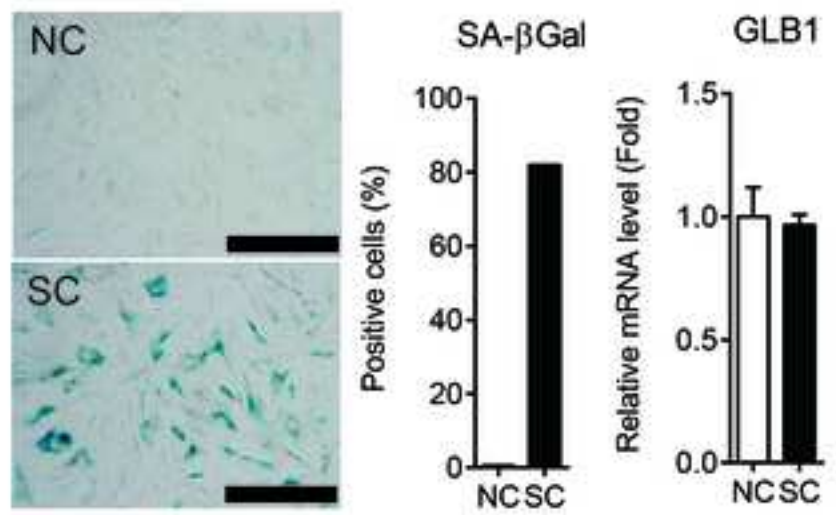
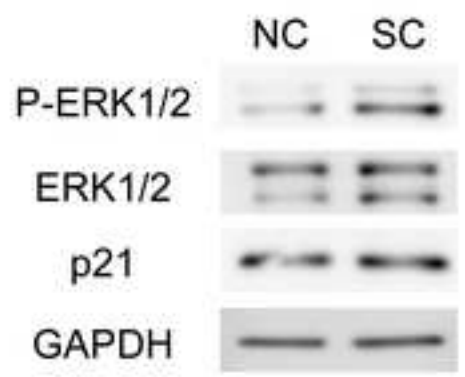


Figure 4

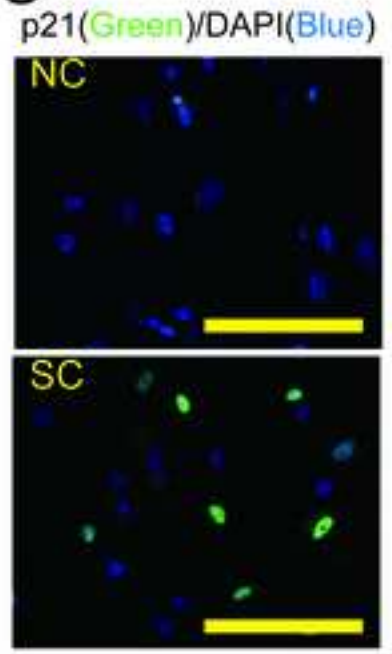
A



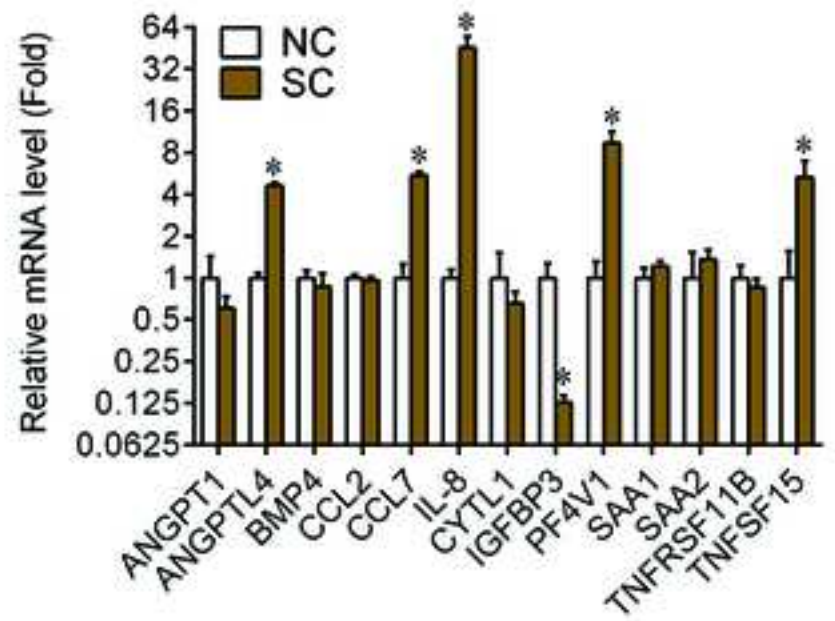
B



C



D



E

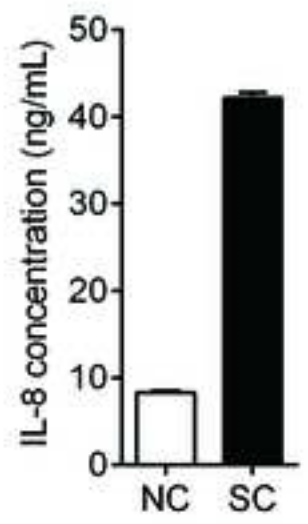
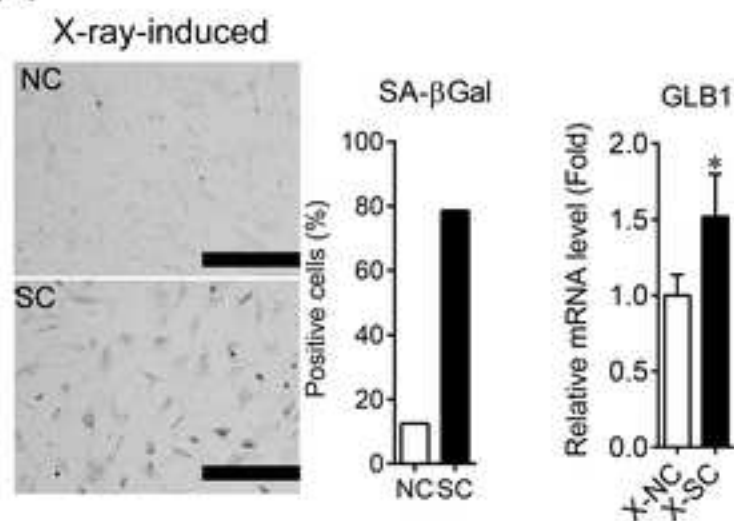


Figure 5

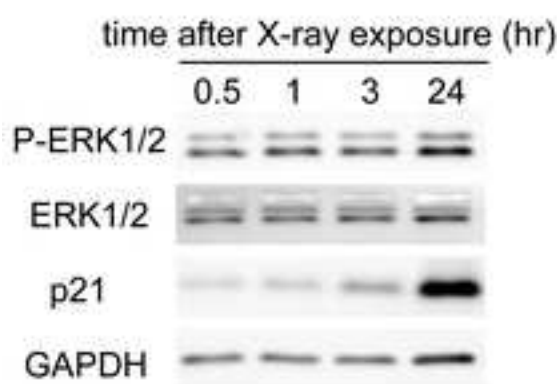
A



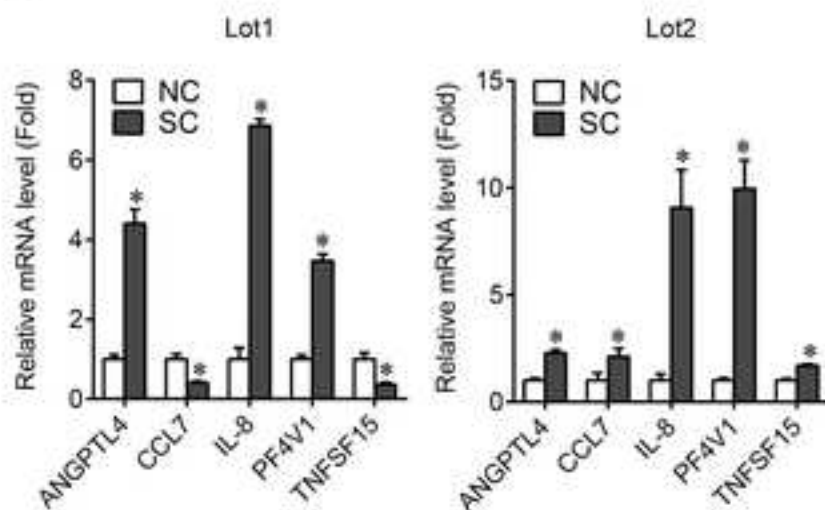
B



C



D



E

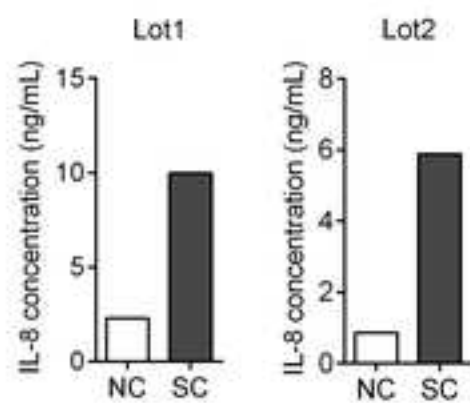


Table 1. Primary antibodies used in this study.

Anti-	Company	Cat. No
p21 ^{Waf1/Cip1}	Cell Signaling Technology	#2947
phospho-MEK1/2	Cell Signaling Technology	#9154
MEK1/2	Cell Signaling Technology	#8727
phospho-ERK1/2	Cell Signaling Technology	#4370
ERK1/2	Cell Signaling Technology	#4695
phospho-p38	Cell Signaling Technology	#4511
p38	Cell Signaling Technology	#8690
phospho-SAPK/JNK	Cell Signaling Technology	#4668
SAPK/JNK	Cell Signaling Technology	#9252
phospho-histone H2AX (γ H2AX)	Cell Signaling Technology	#2577
histone H2AX	Cell Signaling Technology	#7631
CDT1	Abcam	Ab202067
LMNB1	Santa Cruz Biotechnology	SC374015
GAPDH	Millipore	MAB374

Table 2. Primers used in this study.

Gene	Forward (5' to 3')	Reverse (5' to 3')
18S	CAGCCACCCGAGATTGAGCA	TAGTAGCGACGGGCGGTGTG
GLB1	CTCCTTCTGCTGCTGGTTC	GGAGTCCCGGCTATAGTCAA
α SMA	CAGCCAAGCACTGTCAGG	CCAGAGCCATTGTACACAC
COL1A1	AAGAGGAAGGCCAAGTCGAG	CACACGTCTCGGTCATGGTA
COL1A2	GAAAAGGAGTTGGACTTGGC	AGCAGGTCCTTGAAACCTT
PPAR γ	AGGCCATTTTCTCAAACGAG	GAGAGATCCACGGAGCTGAT
CYGB	CGAGATGGAGATCGAGCG	CGAGGGGAAGTTCACAAAGA
IL-8	CAAGAGCCAGGAAGAAACCA	AGCACTCCTTGGCAAAACTG
IL-1 β	GAAGCTGATGGCCCTAAACA	AAGCCCTTGCTGTAGTGGTG
IL-6	AGTGAGGAACAAGCCAGAGC	CATTTGTGGTTGGGTCAGG
SERPINE1	AGAAACCCAGCAGCAGATTC	TGGTGCTGATCTCATCCTTG
VEGF	CTACCTCCACCATGCCAAGT	AGCTGCGCTGATAGACATCC
WFDC1	CTACGCCTGCCTAGAAGCTG	ACGCCTCTGCTTGTAAACACC
CYTL1	TTCAACCTCCTGCAGGTCTC	GGAATCTACCTGGGCCACTT
EDN1	CAAGGAGCTCCAGAAACAGC	TTTATCCATCAGGGACGAGC
PF4V1	GAGATGCTGTTCTTGCGTTC	GGAGGTGGTCTTCACACACA
IGFBP3	AACGCTAGTGCCGTCAGC	GACGGGCTCTCCCACTG
MFGE8	AGATTGTACCCACGAGCTG	GCTGTTATTCTTCAGGCCCA
CFD	TTGATGTGCGCGGAGAG	GAGGTGACCACGCCCTC
CCL7	CTGCTTTCAGCCCCAG	AGCTCTCCAGCCTCTGCTTA
CCL2	GCCTCCAGCATGAAAGTCTC	AGGTGACTGGGGCATTGAT
PSG5	GGAACCTGCCTATCACTGCT	TGTAATGGTAGAGGTCCATCAG
LEPREL1	CGCAGAGTGCCCTACAATA	ATGTGCTCAGGGTTAGCCAC
ANGPT1	ACCGGATTTCTCTTCCCAGA	CCGACTTCATGTTTTCCACA
WNT2B	GACGGCAGTACCTGGCATA	TGTCACAGATCACTCGTGCC
SAA2	TGGTTTTCTGCTCCTTGGTC	GTAGGCTCTCCACATGTCCC
BMP6	CATGAGCTTTGTGAACCTGG	CACCTCACCTCAGGAATCT
TNFRSF11B	GGGGACCACAATGAACAAGT	GCTGATGAGAGGTTTCTTCG
TNFSF15	CACATACCTGCTTGTCAGCC	TGTGAAGGTGCAAACCTCTG
FIBIN	GGCTCAACGAGGACTTTCTG	GCTCGTATTTGTCCCTGAGC

Table 2. Primers used in this study (Continued).

Gene	Forward (5' to 3')	Reverse (5' to 3')
RARRES2	AGAGGGACTGGAAGAAACCC	TTTGTCTCAGAGCCCAGTT
IGF2	CTGTTCGGTTTTCGACAC	CCAAGAAGGTGAGAAGCACC
BMP4	TGAGCCTTCCAGCAAGTTT	GCATTCGGTTACCAGGAATC
ANGPTL4	GAGATGGCCCAGCCAGTT	TAGTCCACTCTGCCTCTCCC
ADM	GCTTGGACTTCGGAGTTTTG	ACGGAAACCAGCTTCATCC
SAA1	AGCCGAAGCTTCTTTTCGTT	GCCGATGTAATTGGCTTCTC

18S, 18 S ribosomal RNA; GLB1, galactosidase beta 1; α SMA, alpha-smooth muscle actin; COL1A1, collagen type I alpha 1; COL1A2, collagen type I alpha 2; PPAR γ , peroxisome proliferator-activated receptor gamma; CYGB, cytoglobin; SERPINE1, serpin family E member 1; WFDC1, WAP four-disulfide core domain 1; CYTL1, cytokine like 1; EDN1, endothelin 1; PF4V1, platelet factor 4 variant 1; IGFBP3, insulin like growth factor binding protein 3; MFGE8, milk fat globule-EGF factor 8 protein; CFD, complement factor D; CCL7, C-C motif chemokine ligand 7; CCL2, C-C motif chemokine ligand 2; PSG5, pregnancy specific beta-1-glycoprotein 5; LEPREL1, prolyl 3-hydroxylase 2; ANGPT1, angiopoietin 1; WNT2B, Wnt family member 2B; SAA2, serum amyloid A2; BMP6, bone morphogenetic protein 6; TNFRSF11B, TNF receptor superfamily member 11b; TNFSF15, TNF superfamily member 15; FIBIN, fin bud initiation factor homolog (zebrafish); RARRES2, retinoic acid receptor responder 2; IGF2, insulin like growth factor 2; BMP4, bone morphogenetic protein 4; ANGPTL4, angiopoietin like 4; ADM, adrenomedullin; SAA1, serum amyloid A1.

Table 3. 25 genes selected from microarray analysis.

Gene Symbol	Description	SC/NC
WFDC1	WAP Four-Disulfide Core Domain 1	193.20
CYTL1	Cytokine Like 1	29.94
EDN1	Endothelin 1	12.50
PF4V1	Platelet Factor 4 Variant 1	10.63
IGFBP3	Insulin Like Growth Factor Binding Protein 3	10.28
MFGE8	Milk Fat Globule-EGF Factor 8 Protein	9.57
CFD	Complement Factor D	9.52
CCL7	C-C Motif Chemokine Ligand 7	9.09
CCL2	C-C Motif Chemokine Ligand 2	8.45
CXCL8 (IL-8)	C-X-C Motif Chemokine Ligand 8 (Interleukin-8)	7.31
PSG5	Pregnancy Specific Beta-1-Glycoprotein 5	6.98
LEPREL1	Leprecan-Like Protein 1	6.59
ANGPT1	Angiopoietin 1	6.57
WNT2B	Wnt Family Member 2B	6.27
SAA2	Serum Amyloid A2	6.11
BMP6	Bone Morphogenetic Protein 6	6.06
TNFRSF11B	Tumor Necrosis Factor Receptor Superfamily, Member 11b	6.05
TNFSF15	Tumor Necrosis Factor Superfamily Member 15	5.63
FIBIN	Fin Bud Initiation Factor Homolog (Zebrafish)	5.54
RARRES2	Retinoic Acid Receptor Responder 2	5.17
IGF2	Insulin Like Growth Factor 2	5.04
BMP4	Bone Morphogenetic Protein 4	4.93
ANGPTL4	Angiopoietin Like 4	4.81
ADM	Adrenomedullin	4.80
SAA1	Serum Amyloid A1	4.59